*Int. J. Heat Mass Transfer.* Vol. 27, No. 3, pp. 327–335, 1984
Printed in Great Britain

0017 9310/84 $3.00 + 0.00
Pergamon Press Ltd.

# A MICROSCOPIC STUDY OF DROPWISE CONDENSATION

HIROAKI TANAKA
Department of Mechanical Engineering, University of Tokyo, Bunkyo-ku, Tokyo, Japan

and

TAKAHARU TSURUTA
Division of Nuclear Safety Research, Japan Atomic Energy Research Institute, Tokai-mura, Ibaraki-ken, Japan

(*Received* 28 *April* 1983 *and in revised form* 10 *June* 1983)

**Abstract**—In dropwise condensation most of the heat is transferred by the active droplets whose sizes are below a certain characteristic value so that the thermal conduction resistance inside them may become negligible. In this paper the local heat transfer coefficient is determined experimentally at the very part of the condenser surface which is covered solely by the active droplets. The rate of increase in the condensate volume in a domain newly exposed by coalescence between droplets was analyzed from a high-speed high-magnification cine film record of the condenser surface. By assuming the complete coverage of the surface by droplets, the local heat transfer coefficient obtained in this way was equated to the interfacial heat transfer coefficient. As a result, the condensation coefficient of water was estimated at around 0.5.

## NOMENCLATURE

| | |
|---|---|
| $Bi$ | Biot number, $h_i R_{max}/\lambda_l$ |
| $Bi_c$ | Biot number, $hR_{max}/\lambda_c$ |
| $\bar{f}$ | time-averaged fraction of the condenser surface covered by active droplets |
| $H$ | distance of wire from the condenser surface |
| $h$ | average heat transfer coefficient of dropwise condensation |
| $h_{fg}$ | latent heat of vaporization |
| $h_i$ | interfacial heat transfer coefficient |
| $h_l$ | local heat transfer coefficient at the newly exposed domain |
| $h_m$ | average heat transfer coefficient, measured |
| $l$ | mean free path |
| $N$ | nucleation-site density |
| $P_s$ | vapor pressure |
| $q$ | heat flux |
| $q_l$ | local heat flux at the newly exposed domain |
| $R$ | gas constant |
| $R_{max}$ | departing drop size |
| $r$ | drop radius |
| $r_1$ | characteristic drop size |
| $S$ | area defined in the newly exposed domain |
| $T_s$ | saturation temperature |
| $\Delta T$ | surface subcooling |
| $t$ | time |
| $V$ | volume of condensate in $S$ |
| $v_g$ | specific volume of the vapor |
| $v_l$ | specific volume of the liquid. |

Greek symbols

| | |
|---|---|
| $\alpha$ | real condensation coefficient |
| $\alpha'$ | apparent condensation coefficient |
| $\lambda_c$ | thermal conductivity of the condenser surface |
| $\lambda_l$ | thermal conductivity of the liquid |
| $\theta_c$ | contact angle of the liquid. |

## 1. INTRODUCTION

THE MECHANISM of dropwise condensation seems to have been fairly elucidated by one of the authors' series of studies [1–4].

In dropwise condensation, the vapor condenses at the surface of each droplet that resides on the condenser surface, and the latent heat of liquefaction is transferred to the condenser surface by thermal conduction inside the droplet.

From the kinetic theory of gases [5, 6], a thermal resistance characterized by the interfacial heat transfer coefficient in equation (1) exists at the liquid–vapor interface, resulting in a droplet surface temperature that is lower than the saturation temperature $T_s$ corresponding to the vapor pressure $P_s$ in the condenser chamber

$$h_i = \frac{2\alpha}{2-\alpha}\frac{1}{(2\pi R T_s)^{1/2}}\frac{h_{fg}^2}{v_g T_s}, \tag{1}$$

where $R$ is the gas constant, $h_{fg}$ the latent heat of vaporization, and $v_g$ the specific volume of the vapor. The condensation coefficient, $\alpha$, is the ratio of the vapor molecules that will be captured by the liquid phase to the total number of the vapor molecules that hit the liquid surface.

A droplet is either active or inactive depending on its radius being smaller or larger than the following characteristic size [3, 7]

$$r_1 = \frac{2\lambda_l}{h_i}, \tag{2}$$

where $\lambda_l$ is the thermal conductivity of the liquid. An active droplet is almost throughout at the same temperature as the condenser surface and the heat transfer rate through it is entirely controlled by the interfacial heat transfer coefficient in equation (1). On

the other hand, an inactive drop acts virtually as an insulator, because the thermal conduction resistance inside it becomes very large. The characteristic size $r_1$ varies with pressure and its actual value ranges from a few tenths of a micrometer to several micrometers as for water and some organic compounds. Thus $r_1$ is roughly three orders of magnitude smaller than the departing drop size $R_{max}$.

As for the size distribution of drops on the condenser surface, a comprehensive theory has been developed [1–3]. From the theory, we can estimate the time-averaged fraction $\bar{f}$ of the condenser surface which can be utilized by the active droplets without being occupied by the inactive drops as [4]

$$\bar{f} = 1.74Bi^{-0.3}, \tag{3}$$

where $Bi$ is the Biot number defined by

$$Bi = \frac{h_i R_{max}}{\lambda_l} = \frac{2R_{max}}{r_1}. \tag{4}$$

For example, when $Bi = 2 \times 10^2$ and $2 \times 10^4$, $\bar{f}$ amounts to 35.5 and 8.9%, respectively. Here, we assume that the nucleation-site density is infinitely high. Then the foregoing fraction $\bar{f}$ of the condenser surface is fully covered by the active droplets (strictly, the condition that the size of the thermodynamic critical drop is effectively zero is further needed).

At this juncture, for the case of water, the magnitude of the mean free path $l$ is almost equivalent to the characteristic drop size $r_1$ [4]. In such a case (more strictly, when condition $r_1 < l$ is fulfilled), as for the very part of the condenser surface which is covered entirely by the active droplets, the liquid–vapor interface formed by the densely populated active droplets is microscopically very complicated indeed, but it can be regarded as a flat surface having the same area as its normal projection, with respect to the interface matter transfer characterized by equation (1). Thus heat is transferred per unit condenser area and per unit time at a rate of $h_i \Delta T \bar{f}$, where $\Delta T$ is the subcooling of the condenser surface. Ultimately, we have for the time-averaged heat transfer coefficient of steady dropwise condensation [4]

$$h = h_i \bar{f}.$$

Namely

$$h/h_i = 1.74Bi^{-0.3}. \tag{5}$$

To sum up, provided the nucleation-site density is infinitely high, we can calculate the interfacial heat transfer coefficient $h_i$ from the experimental data of $h$ and $R_{max}$ with the aid of equation (5), and then we can estimate the condensation coefficient $\alpha$ from equation (1). By following this procedure, the condensation coefficient of water was estimated at around 0.45 in ref. [4].

The distinctive feature of this report is the experimental determination of the local heat transfer coefficient $h_l$ at the very part of the condenser surface which is covered entirely by the active droplets. A great number of coalescences between droplets occur on the condenser surface. Every coalescence yields a bit of bare surface, which is covered by the primary droplets without delay. Thus 'localized transient dropwise condensation' is repeated innumerably on the condenser surface. The localized transient dropwise condensation soon merges into the surroundings, since the area that is newly made bare by coalescence is usually very small. In the present study, the condenser surface was filmed with a high-speed camera through a microscope. A series of frames which successfully caught the localized transient dropwise condensation were selected and analyzed. The local heat transfer coefficient $h_l$ was calculated from the rate of increase in the condensate volume at the newly exposed domain. At the same time, the density of the nucleation sites was examined on still pictures. In the end we presumed the complete coverage of the surface by droplets, and equated the local heat transfer coefficient $h_l$, obtained in the foregoing way, with the interfacial heat transfer coefficient $h_i$. Theoretical results drawn from this assumption are discussed in the last section of this paper.

In the experiment water was used as the test fluid. The experimental pressure $P_s$ was taken as low as possible. This is because the interfacial heat transfer coefficient $h_i$ decreases with decreasing $P_s$. Then, lowering $P_s$, we can get the characteristic drop size $r_1$ in equation (2) larger, which permits the size range of both visible and active droplets to become broader. In addition, the time-averaged heat transfer coefficient of steady dropwise condensation, $h$, decreases with decreasing $P_s$, as is easily understood from equations (4) and (5). The surface temperature of the test condenser having a finite thermal conductivity will not be uniform because of the constriction of the heat flow lines caused by the drop-size distribution [8–10]. This non-uniformity of the surface temperature is moderated with a decrease in the average heat transfer coefficient $h$, as will be discussed later. Therefore, the employment of the lowest possible pressure is desirable also in this respect.

## 2. EXPERIMENTAL APPARATUS

The schematic diagram of the apparatus is shown in Fig. 1. Distilled water was evaporated in the boiler. The generated steam was partially condensed in the test condenser in the dropwise mode, and the remainder went into the secondary condenser. The system pressure $P_s$ was almost determined by the coolant temperature of the secondary condenser. Either cold water or aqueous alcohol cooled by dry ice was employed to cool the test condenser. Control of this coolant temperature permitted the surface subcooling of the test condenser to be adjusted to a desired value.

The setup of the test condenser is shown in Fig. 2. The condenser block was made of copper and its main part had the shape of a cylinder, 18 mm in diameter and 35 mm long (see Fig. 3). The condensing surface was

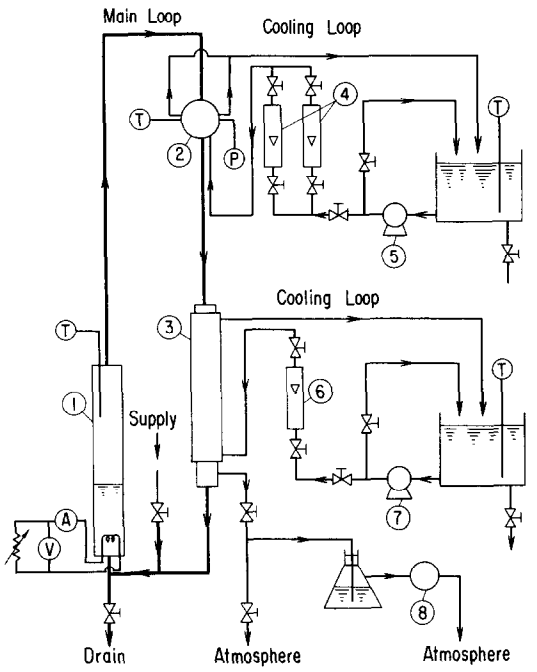


FIG. 1. Schematic diagram of the experimental setup.

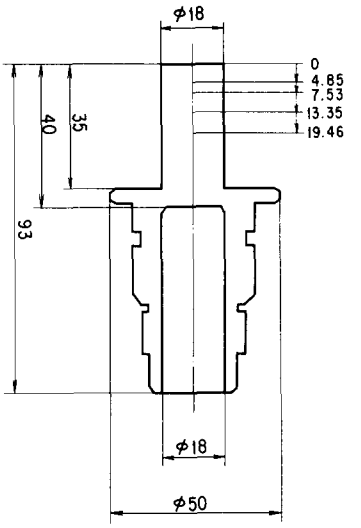


FIG. 3. Condenser block; location of thermocouple holes.

oriented vertical. High-magnification observation was possible through the 3 mm thick glass window which was placed in front of the condenser surface with a space of 3 mm. In order to promote dropwise condensation, the condenser surface was plated with chromium 2.5 $\mu$m thick after it was plated with nickel 5 $\mu$m thick.

Four thermocouple holes, 0.7 mm in diameter, were drilled radially in the axis of the condenser block. Their detailed location is given in Fig. 3. Sheathed, chromel–alumel thermocouples 0.5 mm in diameter were installed in these holes. By applying least square regression to the readings of these thermocouples, a linear temperature distribution in the condenser block was determined. The heat flux $q$ and the surface temperature $T_f$ were respectively obtained from the gradient and from the extrapolation of the temperature distribution. The surface subcooling $\Delta T$ was taken as the difference between the surface temperature $T_f$ and the steam temperature $T_s$ which was measured by the thermocouple located a little downstream of the test surface in the condensing chamber (see Fig. 2).

In order to avoid the effects of non-condensibles, the mean steam velocity in the test condenser was adjusted to about ten times the mean suction velocity toward the condenser surface caused by condensation [11, 12].

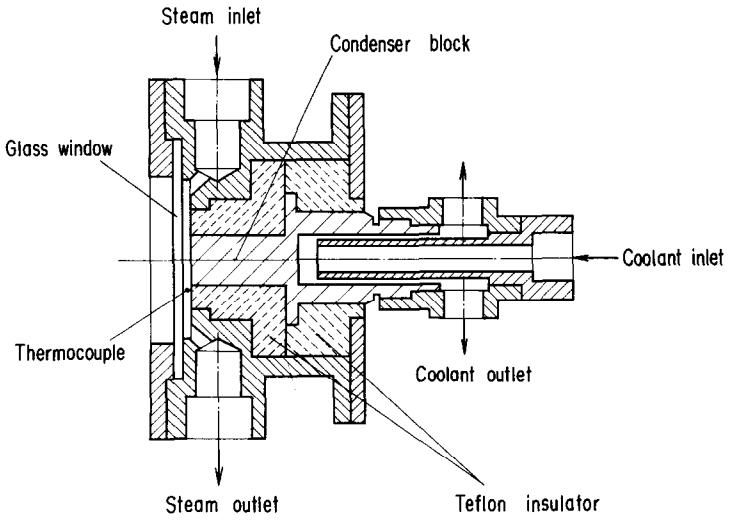


FIG. 2. Test condenser.

The vacuum pump was kept going lest non-condensibles accumulate in the secondary condenser (see Fig. 1).

### 3. MEASUREMENT OF CONTACT ANGLE

Knowledge of the contact angle of the liquid is necessary to calculate the volume of a droplet from its diameter measured from the front-view picture of the condenser surface. The contact angle is determined by the balance of the interfacial energies between the solid and gas phase, solid and liquid phase, and liquid and gas phase, and it is invariable of the drop size [13]. When a force such as gravity acts on a drop, a difference appears between the advancing and receding angles [14]. In the case of a small droplet, however, this difference is so small that the droplet can be assumed to be of the form of a spherical segment. In this preliminary experiment, the contact angle was measured for droplets which were actually growing during dropwise condensation of pure steam on the same test surface at nearly the same pressure as the main experiment.

A fine wire of 20 $\mu$m in diameter was stretched at a constant distance $H$ from the condenser surface. From the cine film record of the front view of the condensing surface, was selected the frame which caught the instant when a growing droplet just came into contact with the wire. By measuring the drop radius $r$ and the distance $d$ between the center of the drop and the contact point from the enlarged picture of the frame, the contact angle $\theta_c$ was found as

$$\tan \theta_c = \frac{2rH}{r^2 - d^2 - H^2} \qquad (\theta_c < 90°), \qquad (6)$$

or

$$\cos \theta_c = \frac{(r^2 - d^2)^{1/2} - H}{r} \qquad (\theta_c \geq 90°). \qquad (7)$$

The distance $H$ of the wire from the condenser surface was determined as follows, by using a microscope with a depth of focus of 3.5 $\mu$m. The focus of the microscope was adjusted first on the wire and then on the condenser surface, and the displacement of the microscope body between the two adjustments was measured with a dial-gauge.

Figure 4 shows the results obtained under the conditions of the saturation temperature $T_s = 290.1$ K, the surface subcooling $\Delta T = 1.21$ K, and the wire distance $H = 0.345$ and 0.455 mm. In the figure the contact angle $\theta_c$ obtained is plotted against the drop radius $r$. The range of $r$ measured extends from the value of $H$ used to 1.2 mm. This corresponds to the departing drop size $R_{max}$. The data of $\theta_c$ lies between 90° and 80°. Taking account of the hysteresis of the contact angle and also the uncertainty in distinguishing the occurrence of contact between the wire and the drop, the data obtained for drops with radii a little larger than $H$ are most reliable. If we assume the uncertainty of $H$ to be $\pm 20$ $\mu$m which corresponds to the wire diameter, the calculated result of $\theta_c$ includes the uncertainty of $\pm 3°$.

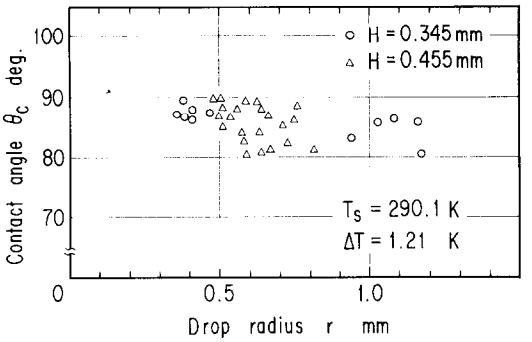


FIG. 4. Measured results of contact angle.

In conclusion, it seems reasonable to assume that the contact angle of droplets on the chromium-plated surface used in this experiment is 90°.

### 4. OBSERVATION OF THE LOCALIZED TRANSIENT CONDENSATION

Measurements were carried out for the two cases shown in Table 1. By the reason described in the Introduction, the experimental pressure $P_s$ was taken as low as possible, and was set to 1.57 and 1.18 kPa. The surface subcooling $\Delta T$ was set at around 2 K in order that the potential nucleation site might be fully activated. In the fourth line of Table 1 is listed the space-averaged heat transfer coefficient $h_m = q/\Delta T$, where for the heat flux $q$ and the subcooling $\Delta T$ were used the values obtained from the temperature distribution in the condenser block. Figure 5 shows the available experimental results of the heat transfer coefficient for dropwise condensation of steam at pressures below 1 atm [15–18]. In this figure, the data of the present investigation are also plotted.

A microscope equipped with a long work-distance object lens (7.7 mm work-distance, 40 × magnification

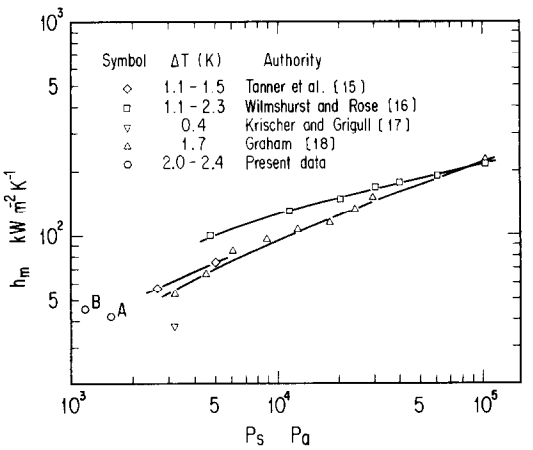


FIG. 5. Heat transfer coefficient at low pressures.

Table 1. Summary of experiment

| Case | | A | B |
|---|---|---|---|
| $T_s$ | (K) | 286.91 | 283.09 |
| $P_s$ | (kPa) | 1.568 | 1.176 |
| $\Delta T$ | (K) | 2.00 | 2.39 |
| $h_m$ | (kW m$^{-2}$ K$^{-1}$) | 41.49 | 45.24 |
| $(\Delta V/\Delta t)/S$ | (m s$^{-1}$) | $1.776 \times 10^{-4}$ | $1.506 \times 10^{-4}$ |
| $h_l$ | (kW m$^{-2}$ K$^{-1}$) | 219.3 | 156.1 |
| $\alpha'$ | | 0.570 | 0.517 |
| $\alpha$ | | 0.50 | 0.45 |
| $Bi = h_l R_{max}/\lambda_l$ | | 443.2 | 319.1 |
| $\bar{f}$ | | 0.280 | 0.308 |
| $h$ | (kW m$^{-2}$ K$^{-1}$) | 61.40 | 48.08 |
| $r_1$ | ($\mu$m) | 5.40 | 7.52 |
| $l$ | ($\mu$m) | 2.6 | 3.3 |
| $(l/r_1)^{0.3}$ | | 0.80 | 0.78 |

and 0.7 $\mu$m resolution) was employed. The central part of the condenser surface was filmed through the microscope by a high-speed camera at the rate of 3000 frames per second. A mercury lamp was used for illumination. The recorded film was analyzed as follows. The frame which fixed the instant when a bare bit of surface was just exposed by coalescence between droplets was sought out. The time $t$ was counted from that frame. A rectangular space $S$ of 200–900 $\mu$m$^2$ in size was defined within the newly exposed domain. Every frame or at intervals of one to two frames, all droplets inside the space $S$ were counted and measured. The measurement started from the frame on which droplets were already discernible everywhere in the space $S$ with the diameters having grown over the resolution of the microscope. It was continued until the size of the largest droplet in the space $S$ exceeded a radius of 5 $\mu$m.

From the result of the preliminarly experiment, we assumed the droplets to be hemispherical, and calculated the total volume $V$ of condensate in the space $S$. The condensate volume per unit area of the newly exposed domain, $V/S$, varied with the time $t$ as plotted in Figs. 6 and 7, which correspond to Cases A and B in Table 1, respectively. Figures 5 and 6 show four kinds of symbols, which represent four distinct occurrences of the localized transient condensation, observed at different places and different times within a fixed field of vision. In the course of the transient condensation, a droplet would often go out of the space $S$ by coalescence with a drop outside of $S$, while another would come into $S$ from outside. In the former case the volume of the leaving droplet was added to $V$ from that time on, whereas in the latter case the volume of the entering droplet was deducted from $V$. The size of $S$ was naturally restricted by the extent of the newly exposed domain. When a larger size of $S$ was employed, the foregoing correction of $V$ due to entering or leaving droplets became relatively smaller, but a longer time had to elapse until droplets became discernible throughout $S$. It is worth noting that the error of $V$ due to the omission of droplets smaller than the resolving

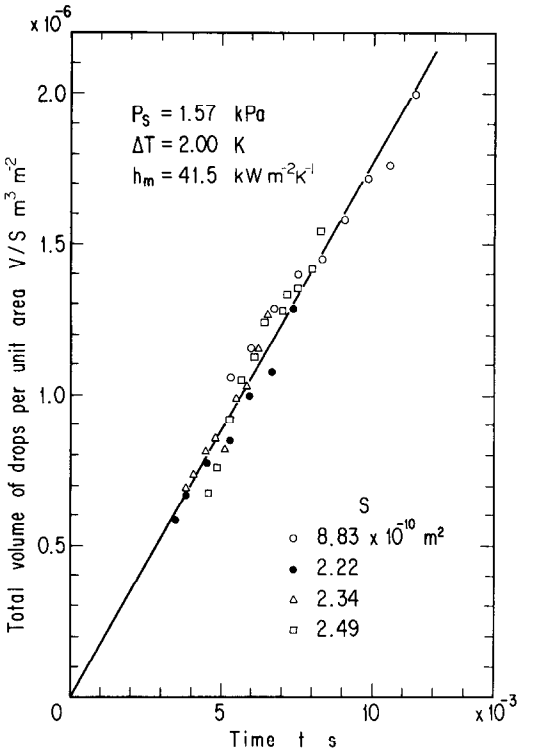


FIG. 6. Variation of volume of condensate with time, Case A.

power was negligible because a droplet has a volume proportional to the third power of its radius.

The straight lines in Figs. 6 and 7 were drawn by the least square regression for the data points. The data

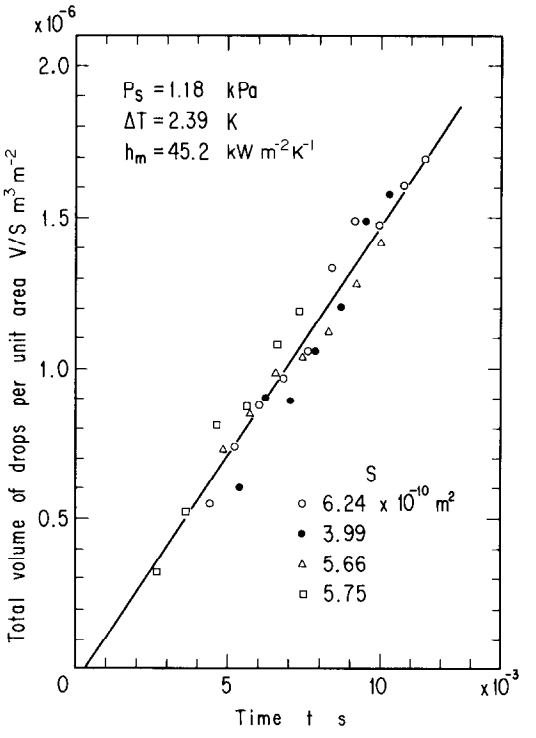


FIG. 7. Variation of volume of condensate with time, Case B.

follow these lines very well. In addition the extension of these lines passes the origin of the coordinates within the tolerance corresponding to the time interval between neighboring frames of the high-speed cine film. The gradients of these lines $(\Delta V/\Delta t)/S$ are listed in the fifth line of Table 1. If the local heat flux is estimated by

$$q_l = \frac{h_{fg}}{v_l}\frac{1}{S}\left(\frac{\Delta V}{\Delta t}\right), \tag{8}$$

where $v_l$ is the specific volume of the liquid, the local heat transfer coefficient $h_l$ can be calculated by

$$h_l = \frac{q_l}{\Delta T}. \tag{9}$$

The sixth line of Table 1 gives $h_l$ obtained in this way.

For calculating $h_l$ from equation (9) we were compelled to make use of the surface subcooling $\Delta T$ which was obtained from the linear extrapolation of the temperature distribution in the condenser block. Here, we examine the uniformity of the condenser surface temperature. A series of papers has been published by Mikic and his co-workers [8–10] on the constriction resistance in the dropwise-condensation heat transfer. This resistance arises from the constriction of the heat flow lines, correspondingly, from the non-uniformity of the surface temperature, caused by the drop-size distribution. It is suspected that, in the case of condensation of steam on the copper surface, the constriction resistance is tolerably small compared with the thermal resistance on the steam side even in the case of condensation at atmospheric pressure [9, 10], where the steam-side heat transfer coefficient is five times as large as that in the present experiment. It seems to be admitted that the importance of the constriction resistance relative to the steam-side thermal resistance decreases with an increase in the thermal conductivity of the condenser surface as well as with a decrease in the heat transfer coefficient of dropwise condensation. In this place it is conjectured that the constriction resistance is characterized by the Biot number $Bi_c = hR_{max}/\lambda_c$, where $h$ is the heat transfer coefficient of dropwise condensation, $R_{max}$ is the radius of the departing drop, and $\lambda_c$ is the thermal conductivity of the condenser surface. For the present experimental conditions, we have $Bi_c = h_m R_{max}/\lambda_c = 0.13$. This means that the thermal conductance of a copper plate of $R_{max}$ in thickness, $\lambda_c/R_{max}$, is about eight times as large as the thermal conductance on the steam side, $h_m$. Here, it is supposed that the drop-size distribution with the characteristic scale of $R_{max}$ causes the heat-flux distribution inside the condenser surface to be disturbed within the surface layer of $R_{max}$ in thickness. Then, the amplitude of the surface temperature variation is considered to be of the order of one-tenth of the average surface subcooling $\Delta T$.

## 5. DISCUSSION

As for the nucleation-site density $N$ on the condenser surface, McCormick and Westwater [19] reported the value of the order of $10^9$ sites $m^{-2}$ during dropwise condensation of steam at room temperature on a copper surface promoted with benzyl mercaptan. Krischer and Grigull [17] carried out an experiment on dropwise condensation of steam at about 25°C on copper and brass surfaces promoted with silicon oil. They reported that the nucleation-site density $N$ increased with the increase in the surface subcooling $\Delta T$, coming up to about $1.6 \times 10^{10}$ sites $m^{-2}$ at $\Delta T = 0.4$ K. Tanasawa and Nagata [20], by making use of a technique in an electron microscope, investigated the primary-drop formation on a cold glass plate exposed to moist air. The value they obtained was as high as $2.6 \times 10^{15}$ drops $m^{-2}$. Graham and Griffith [18] studied dropwise condensation of steam on a copper surface promoted with dioctadecyl disulphide in the range of steam temperature $T_s$ from 25 to 100°C. They reported that for the surface subcooling of $\Delta T = 0.28$ K the nucleation-site density $N$ was measured to be $2 \times 10^{12}$ sites $m^{-2}$ at $T_s = 31.1$°C and that at $T_s = 100$°C $N$ increased by a factor of about three for the same subcooling. (Afterwards, they revised the value to $N \simeq 6 \times 10^{11}$ sites $m^{-2}$ [21].) Of these works, Krischer and Grigull, and Graham and Griffith measured the heat transfer coefficient simultaneously. The results are included in Fig. 5. In this figure Krischer and Grigull's experimental point is somewhat lower than others. This seems to be related to the fact that their experimental value of $N$ was relatively low.

For each of the eight samples of the localized transient dropwise condensation analyzed and plotted in Figs. 6 and 7, the density of visible droplets in the defined space $S$, counted on the first frame from which we could start measurement, ranged from $5 \times 10^{10}$ to $1.2 \times 10^{11}$ drops $m^{-2}$. Correspondingly the mean spacing between droplets was from 4.5 to 2.9 $\mu$m. In the high-speed motion pictures, it was feared that coalescence between droplets would occur within the exposure time per frame and obscure the image. So, besides high-speed filming, we took a number of instantaneous pictures using a stroboscope in order to make good use of the resolving power of the microscope. From the pictures which caught the first stage of the localized transient dropwise condensation with success, the droplets were found to be populated so densely to the best of the resolving power, with the minimum distinguishable mean spacing being about 1 $\mu$m. But the questions: how the droplets were distributed before becoming visible and how the space between visible droplets was, could not help but remain unsolved. Through the foregoing optical study, however, we were inclined to consider that under the present experimental conditions with the surface subcooling of $\Delta T \simeq 2$ K the active nucleation-site density was so high that the condenser surface was completely covered by droplets.

Provided the nucleation-site density is infinitely high, we can equate the interfacial heat transfer coefficient $h_i$ in equation (1) to the local heat transfer coefficient $h_l$ at the domain which is covered solely by

droplets smaller than the characteristic size $r_1$ of equation (2), as explained in the Introduction. It will be examined in the last part of this section whether or not the largest droplet in the specified space $S$ remained below $r_1$ in size during the time span in Figs. 6 and 7. Hereupon, the condensation coefficient $\alpha$ was calculated by substituting $h_l$ from Table 1 for $h_i$ in equation (1). The results are listed as $\alpha'$ in the seventh line of Table 1.

The condensation coefficient $\alpha'$ obtained above is in reality an apparent one which should be distinguished from the real condensation coefficient $\alpha$, because the actual liquid–vapor interface has irregularities formed by droplets though the magnitude of the irregularities is assumed to be smaller than the mean free path $l$. The situation is quite similar to the relation between the real and apparent emissivities in the case of thermal radiation for a rough surface [22]. If $\alpha = 1$, then $\alpha' = 1$. When $\alpha < 1$, $\alpha'$ will be a little larger than $\alpha$. The relation between $\alpha$ and $\alpha'$ brings up a rather complicated problem. In the Appendix the problem is solved by approximating the configuration of droplets with a two-dimensional model, consisting of an arrangement of equi-sized semicylinders. By applying the results of this approximation, shown in Fig. A2, the real condensation coefficient $\alpha$ was estimated. The eighth line of Table 1 gives the results.

By equating $h_l$ to $h_i$, we can, on the other hand, predict the space-averaged heat transfer coefficient $h$ from equation (5). The Biot number defined by equation (4) is in the ninth line of Table 1. The time-averaged fraction $\bar{f}$ of the condenser surface which is covered by the active droplets in the size range $r < r_1$ can be calculated from equation (3), and is listed in the tenth line of Table 1. Finally, multiplying $\bar{f}$ by $h_i$ $(= h_l)$ yields the space-averaged heat transfer coefficient $h$, found in the eleventh line of Table 1. The predicted values are in fair agreement with the measured heat transfer coefficient, $h_m$, in the fourth line of Table 1.

In the end, by equating $h_l$ with $h_i$ again, the characteristic size $r_1$ in equation (2) was calculated, as listed in the twelfth line of Table 1. As mentioned previously, in the reduction of the data plotted in Figs. 6 and 7 the measurement of droplet sizes was stopped when the maximum droplet in the specified space $S$ exceeded a radius of 5 $\mu$m. Therefore, the foregoing condition that the space $S$ should be covered solely by droplets smaller than $r_1$ is now proved to have been satisfied.

In this place, the mean free path $l$ in the respective experimental conditions is given in the thirteenth line of Table 1 [23]. It is noted that $r_1$ is greater than $l$. Then, the condition assumed in deriving equation (5) and mentioned just prior to it does not hold strictly true for the droplets having sizes between $l$ and $r_1$. In the same way as equation (3) has been derived, however, it can be shown that, among the surface area which is covered by the active droplets below $r_1$ in size, the droplets smaller than $l$ occupies a fraction $(l/r_1)^{0.3}$. This fraction is given in the last line of Table 1. The percentage seems to be tolerably high for the argument in this section to make sense.

## 6. CONCLUSIONS

High-speed high-magnification observations were performed during dropwise condensation of steam on a chromium-plated copper surface. The experimental pressures were 1.18 and 1.57 kPa, and the surface subcooling was set at about 2 K. The localized transient dropwise condensation, which took place innumerably on the condenser surface in every domain that was exposed bare by coalescence between droplets, was investigated, and the local heat transfer coefficient $h_l$ during the transient condensation in a newly exposed domain was determined. During the observation of the transient condensation which was continued until the largest droplet in the newly exposed domain grew to a radius of 5 $\mu$m, $h_l$ seemed to remain constant, and its magnitude was greater than the space-averaged heat transfer coefficient $h_m$ by a factor of 3.5–5. The value of 5 $\mu$m was shown to be smaller than the characteristic size $r_1$. To the best of the resolving power of the microscope, the condenser surface seemed to be completely covered by droplets. Then, by equating $h_l$ with the interfacial heat transfer coefficient $h_i$, the condensation coefficient of water was estimated at around 0.5. Further, by letting $h_i$ be equal to $h_l$, the space-averaged heat transfer coefficient was predicted from one of the authors' previous theories. The predicted results showed fair agreement with the experimental ones.

*Acknowledgements*—The authors wish to acknowledge Prof. T. Ueda for his instructive comments during this work. They would like to thank Mr S. Hatamiya for his assistance. This work was partly supported by the Ministry of Education of the Japanese Government through a Grant in Aid for Scientific Research, Project No. 57460093.

## REFERENCES

1. H. Tanaka, A theoretical study of dropwise condensation, *Trans. Am. Soc. Mech. Engrs*, Series C, *J. Heat Transfer* **97**, 72–78 (1975).
2. H. Tanaka, Measurements of drop-size distributions during transient dropwise condensation, *Trans. Am. Soc. Mech. Engrs*, Series C, *J. Heat Transfer* **97**, 341–346 (1975).
3. H. Tanaka, Further developments of dropwise condensation theory, *Trans. Am. Soc. Mech. Engrs*, Series C, *J. Heat Transfer* **101**, 603–611 (1979).
4. H. Tanaka, Effect of Knudsen number on dropwise condensation, *Trans. Am. Soc. Mech. Engrs*, Series C, *J. Heat Transfer* **103**, 606–607 (1981).
5. R. W. Schrage, *A Theoretical Study of Interphase Mass Transfer*. Columbia University Press, New York (1953).
6. W. M. Rohsenow, Status of and problems in boiling and condensation heat transfer, in *Progress in Heat and Mass Transfer* (edited by G. Hetsroni *et al.*), Vol. 6, pp. 1–44. Pergamon Press, New York (1972).
7. A. Umur and P. Griffith, Mechanism of dropwise condensation, *Trans. Am. Soc. Mech. Engrs*, Series C, *J. Heat Transfer* **87**, 275–282 (1965).
8. B. B. Mikic, On mechanism of dropwise condensation, *Int. J. Heat Mass Transfer* **12**, 1311–1323 (1969).

9. R. J. Hannemann and B. B. Mikic, An analysis of the effect of surface thermal conductivity on the rate of heat transfer in dropwise condensation, *Int. J. Heat Mass Transfer* **19,** 1299–1307 (1976).
10. R. J. Hannemann and B. B. Mikic, An experimental investigation into the effect of surface thermal conductivity on the rate of heat transfer in dropwise condensation, *Int. J. Heat Mass Transfer* **19,** 1309–1317 (1976).
11. D. W. Tanner, C. J. Potter, D. Pope and D. West, Heat transfer in dropwise condensation—Part I, the effects of heat flux, steam velocity and non condensable gas concentration, *Int. J. Heat Mass Transfer* **8,** 419–426 (1965).
12. I. Tanasawa, J. Ochiai, Y. Utaka and S. Enya, Experimental study on dropwise condensation (effect of departing dropsize), *Trans. Japan Soc. Mech. Engrs* **42,** 2846–2853 (1976).
13. N. K. Adam, *The Physics and Chemistry of Surfaces.* Oxford (1930).
14. N. Fatica and D. L. Katz, Dropwise condensation, *Chem. Engng Prog.* **45,** 661–674 (1949).
15. D. W. Tanner, D. Pope, C. J. Potter and D. West, Heat transfer in dropwise condensation at low steam pressures in the absence and presence of non-condensable gas, *Int. J. Heat Mass Transfer* **11,** 181–190 (1968).
16. R. Wilmshurst and J. W. Rose, Dropwise condensation—further heat-transfer measurements, *Proc. 4th Int. Heat Transfer Conf.*, Paris, Vol. 6, Paper No. Cs 1.4 (1970).
17. S. Krischer and U. Grigull, Mikroskopische Untersuchung der Tropfenkondensation, *Wärme- und Stoffübertragung* **4,** 48–59 (1971).
18. C. Graham and P. Griffith, Drop size distributions and heat transfer in dropwise condensation, *Int. J. Heat Mass Transfer* **16,** 337–346 (1973); also, C. Graham, The limiting heat transfer mechanisms of dropwise condensation, Ph.D. thesis, Massachusetts Institute of Technology (1969).
19. J. L. McCormick and J. W. Westwater, Nucleation sites for dropwise condensation, *Chem. Engng Sci.* **20,** 1021–1036 (1965).
20. I. Tanasawa and S. Nagata, Generation of primary droplets in dropwise condensation, *Prepr. Japan Soc. Mech. Engrs* No. 710-14, 137–140 (1971).
21. L. Glicksman, C. Graham, P. Griffith and A. Hunt, Letter to the editors, *Int. J. Heat Mass Transfer* **16,** 1822 (1973).
22. E. M. Sparrow and V. K. Jonsson, Absorption and emission characteristics of diffuse spherical enclosures, *Trans. Am. Soc. Mech. Engrs*, Series C, *J. Heat Transfer* **84,** 188–189 (1962).
23. E. H. Kennard, *Kinetic Theory of Gases.* McGraw-Hill, New York (1938).
24. E. R. G. Eckert and R. M. Drake, *Analysis of Heat and Mass Transfer*, pp. 511–521 and 568. McGraw-Hill, New York (1972).
25. E. M. Sparrow, Radiant absorption characteristics of concave cylindrical surfaces, *Trans. Am. Soc. Mech. Engrs*, Series C, *J. Heat Transfer* **84,** 283–293 (1962).
26. M. Jakob, *Heat Transfer*, Vol. II, p. 19. Wiley, New York (1957).


## APPENDIX

In case the Knudsen number $l/r$ is large compared to unity, heat and mass exchange between the vapor and the droplets can be treated as free-molecule flow. Then, the situation becomes quite similar to the radiative heat transfer process, with the condensation coefficient corresponding to the absorptivity [24]. The configuration of droplets is now approximated by the two-dimensional arrangement of equi-sized semicylinders, as shown in Fig. A1. The molecular flux $J(\theta)$ incident on the typical surface element $dA$, located at the angular position $\theta$, is expressed by equation (A1) [25]. The

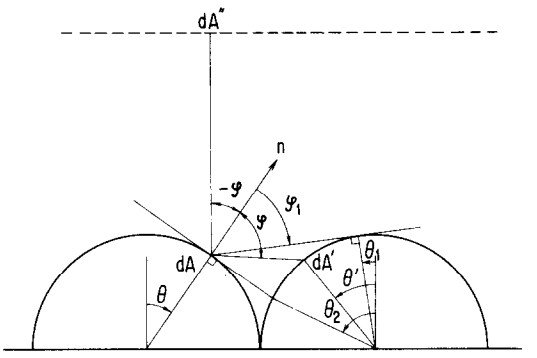


FIG. A1. Two-dimensional model of droplet configuration.

first term on the RHS of equation (A1) represents the molecular flux incident directly from the vapor phase; the second term is the total contribution of molecules reflected to $dA$ from the surface (a typical element is $dA'$ in Fig. A1) of the neighboring droplet; and the third term is the contribution of molecules that reach $dA$ from among ones emitted from the neighboring droplet

$$J(\theta) = \int_{\varphi=-\pi/2}^{\varphi_1} E\, dF_{dA-dA'} + \int_{\theta'=\theta_1}^{\theta_2} (1-\alpha)J(\theta')\, dF_{dA-dA'} + \int_{\theta'=\theta_1}^{\theta_2} \alpha W_+(\theta')\, dF_{dA-dA'}, \quad \text{(A1)}$$

where $dF_{dA-dA'}$ is the shape factor of the area element $dA$ toward $dA'$; $E$ is the number of molecules that travel from the vapor side through the plane parallel to, and at a distance $l$ from, the condenser surface, per unit area and per unit time; $\alpha$ is the real condensation coefficient, and the reflection at the surface is assumed to be diffuse; and $W_+(\theta')$ denotes the molecular flux of the vapor phase which is in thermal equilibrium with the surface element at $\theta'$. By using the relation [26] $dF_{dA-dA'} = \frac{1}{2}\, d(\sin\varphi)$ and assuming the surface temperature to be uniform, equation (A1) becomes

$$J(\theta) = \frac{E}{2}(1+\sin\varphi_1) + (1-\alpha)\int_{\theta'=\theta_1}^{\theta_2} J(\theta')\, dF_{dA-dA'} + \frac{\alpha W_+}{2}(1-\sin\varphi_1). \quad \text{(A2)}$$

The solution of the above integral equation can be expressed as

$$J(\theta) = W_+ + (E - W_+)H(\theta), \quad \text{(A3)}$$

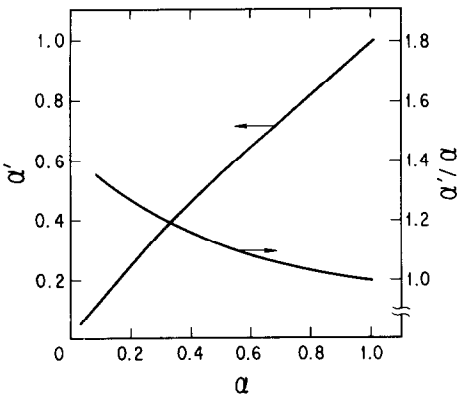


FIG. A2. Relation between apparent and real condensation coefficients.

where $H$ is the solution of

$$H(\theta) = \tfrac{1}{2}(1+\sin\varphi_1)+(1-\alpha)\int_{\theta'=\theta_1}^{\theta_2} H(\theta')\,\mathrm{d}F_{\mathrm{d}A-\mathrm{d}A'}. \quad \text{(A4)}$$

The net condensation rate $W(\theta)$ at the angular position $\theta$ becomes

$$W(\theta) = \alpha J(\theta)-\alpha W_+ = \alpha(E-W_+)H(\theta). \quad \text{(A5)}$$

Finally, the apparent condensation coefficient $\alpha'$ is determined as

$$\alpha' = \int_0^{\pi/2} W(\theta)\,\mathrm{d}\theta/(E-W_+) = \alpha\int_0^{\pi/2} H(\theta)\,\mathrm{d}\theta. \quad \text{(A6)}$$

Equation (A4) was solved numerically for the configuration in Fig. A1, resulting in the relation between $\alpha'$ and $\alpha$, shown in Fig. A2.

## UNE ETUDE MICROSCOPIQUE DE LA CONDENSATION EN GOUTTES

**Résumé**—Dans la condensation en gouttes, la plupart de la chaleur est transférée par les gouttelettes actives dont la taille est inférieure à une certaine valeur caractéristique, de façon que la résistance thermique de conduction à l'intérieur soit négligeable. Dans ce texte, le coefficient de transfert thermique local est déterminé expérimentalement sur la plus grande partie de la surface du condenseur qui est couverte par des gouttelettes actives. La méthode utilisée qui est celle du temps pour la vitesse de croissance dans le volume de condensat dans un domaine nouvellement exposé par coalescence de gouttes, est analysée à partir d'un film à grande vitesse et à grand grossissement. En supposant le recouvrement complet de la surface par les gouttes, le coefficient de transfert thermique local ainsi obtenu est égalé au coefficient de transfert interfacial. Le coefficient de condensation de l'eau est ainsi estimé à 0,5 environ.

## MIKROSKOPISCHE UNTERSUCHUNG DER TROPFENKONDENSATION

**Zusammenfassung**—Bei der Tropfenkondensation wird Wärme überwiegend durch die aktiven Tropfen übertragen, deren Größe unterhalb eines gewissen charakteristischen Werts liegt, wobei der Wärmeleitwiderstand in diesen Tropfen vernachlässigbar wird. In dieser Arbeit wurde der örtliche Wärmeübergangskoeffizient an den Teilen der Kondensatoroberfläche, die nur von diesen aktiven Tropfen bedeckt sind, experimentell bestimmt. Das angewandte Verfahren bestand darin, daß der zeitliche Anstieg des Kondensatvolumens auf einer durch Koaleszenz der Tropfen freigewordenen Fläche mit Hilfe einer stark vergrößerten Hochgeschwindigkeitsfilmaufnahme der Kondensatoroberfläche bestimmt wurde. Unter der Annahme vollständiger Bedeckung der Oberfläche mit Tropfen wurde der örtliche Wärmeübergangskoeffizient, der auf diese Weise erhalten wurde, mit dem Grenzflächen-Wärmeübergangskoeffizienten gleichgesetzt. Auf diese Weise wurde für die Kondensationszahl von Wasser ein Wert von *ca.* 0,5 berechnet.

## МИКРОСКОПИЧЕСКОЕ ИССЛЕДОВАНИЕ КАПЕЛЬНОЙ КОНДЕНСАЦИИ

**Аннотация**—При капельной конденсации бóльшая часть тепла переносится активными каплями, размеры которых меньше определенной характеристической величины, так что тепловым сопротивлением внутри капель можно пренебречь. Экспериментально определяется локальный коэффициент теплопереноса на части поверхности конденсатора, покрытой только активными пузырьками. Сущность используемого метода заключается в том, что интенсивность накопления конденсата в области поверхности, на которой происходит слияние пузырьков, анализируется по кадрам высокоскоростной киносъемки, сделанным с большим увеличением. Коэффициенты локального теплопереноса, полученные в предположении полного покрытия поверхности пузырьками, приравниваются коэффициенту теплопереноса на границе раздела фаз. В результате показано, что коэффициент конденсации для воды равен примерно 0,5.